Spectroscopic Confirmation of Faint Lyman Break Galaxies at Redshifts Four and Five in the Hubble Ultra Deep Field

James E. Rhoads[1,9], Sangeeta Malhotra[1], Norbert Pirzkal[2], Mark Dickinson[3], Seth Cohen[1], Norman Grogin[1,2], Nimish Hathi[1], Chun Xu[2], and the PEARS team

ABSTRACT

We present the faintest spectroscopically confirmed sample of $z \sim 5$ Lyman break galaxies to date. The sample is based on slitless grism spectra of the Hubble Ultra Deep Field region from the GRAPES (Grism ACS Program for Extragalactic Science) and PEARS (Probing Evolution and Reionization Spectroscopically) projects, using the G800L grism on the HST Advanced Camera for Surveys. We report here confirmations of 39 galaxies, pre-selected as candidate Lyman break galaxies using photometric selection criteria. We compare a "traditional" V-dropout selection to a more liberal one (with $V - i > 0.9$), and find that the traditional criteria are about 64% complete and 81% reliable. We also study the Lyman-α emission properties of our sample. We find that Lyman-α emission is detected in $\sim 1/4$ of the sample, and that our broad-band color selected sample includes $\sim 55\%$ of previously published line-selected Lyman-α sources. Finally, we examine our stacked 2D spectra. We demonstrate that strong, spatially extended ($\sim 1''$) Lyman-α emission is not a generic property of these Lyman break galaxies, but that a modest extension of the Lyman-α photosphere (compared to the starlight) may be present in those galaxies with prominent Lyman-α emission.

Subject headings: galaxies: high redshift — galaxies: formation — galaxies: starburst

1. Introduction

Star forming galaxies in the early universe have been found in large numbers both by looking for strong Lyman breaks, and by looking for Lyman-α line emission. Galaxies

---

[1]Arizona State University

[2]Space Telescope Science Institute

[3]National Optical Astronomy Observatory

[9]Email: James.Rhoads@asu.edu

found by these two methods differ greatly in their typical properties. This may indicate physically distinct galaxy populations, or selection effects inherent in the search methods, or a combination of the two. To help address these issues, we here examine the selection of Lyman break galaxies in the Hubble Ultra Deep Field (HUDF). The depth of the HUDF images means that Lyman-α emitting galaxies with fluxes typical of present surveys should all be detected (down to flux $10^{-17}\,\mathrm{erg\,cm^{-2}\,s^{-1}}$), even if they have no continuum emission at all. We combine these deep HUDF images with the deepest slitless spectra ever obtained, from the GRAPES and PEARS projects (see below). These slitless spectra allow us to look for prominent Lyman-α line emission, with or without pre-selection for a Lyman break. We study the continuum properties of a set of Lyman-α selected galaxies, to see what fraction pass our Lyman break crieteria. Conversely, we also study the emission line properties of a Lyman break selected sample. Moreover, we examine spectra for Lyman break samples selected with two sets of photometric criteria, one "traditional" and the other more inclusive.

The Grism ACS Program for Extragalactic Science (GRAPES) project and Probing Evolution And Reionization Spectroscopically (PEARS) project are slitless spectroscopic surveys that exploit the potential of the G800L grism on the Hubble Space Telescope's Advanced Camera for Surveys (ACS) to achieve the most sensitive unbiased spectroscopy yet at red optical wavelengths ($0.58\mu m \lesssim \lambda \lesssim 0.96\mu m$). Two primary factors enhance our sensitivity relative to ground-based spectrographs. First, high redshift galaxies are typically compact (e.g., Ferguson et al 2004; Pirzkal et al 2007; Hathi, Malhotra, & Rhoads 2008), so that the sensitivity of ground-based observations is hampered by atmospheric blurring of the galaxy images (and also usually by slit losses). Second, the OH emission line forest in the night sky spectrum raises the background level for ground-based observations, introducing random noise (and often systematic residuals as well) in red-light spectra of high redshift galaxies from the ground. Our HST spectra are free of both effects. Moreover, because the ACS grism is a slitless spectrograph, we obtain spectra of every source in our field of view, with no preselection required.

GRAPES was targeted in the HUDF region, to complement the HUDF direct images, which are in turn the deepest optical imaging to date (Beckwith et al. 2006). The GRAPES survey, and in particular our data analysis methods, are described in more detail by Pirzkal et al. (2004). PEARS (further described in Malhotra et al 2008) included an additional forty orbits of G800L integration on the HUDF, essentially doubling the integration time. A primary scientific goal of both surveys is to study the properties of Lyman break galaxies using spectroscopically confirmed samples at unprecedented sensitivity. We are pursuing this effort through a targeted look at Lyman break candidates identified in the HUDF using both an i dropout criterion (Malhotra et al 2005) and a V dropout criterion (this paper).

We refer to ACS filters by names of roughly corresponding ground-based filters: F435W $\rightarrow$ B; F606W $\rightarrow$ V; F775W $\rightarrow$ i; and F850LP $\rightarrow$ z. Throughout this paper we use the current concordance cosmology ($H_0 = 71 \, \mathrm{km \, s^{-1} \, Mpc^{-1}}$, $\Omega_M = 0.27$, $\Omega_{total} = 1$; see Spergel et al. 2003, 2007). We use AB magnitudes, so that magnitude zero corresponds to $f_\nu = 3.6 \mathrm{kJy} = 3.6 \times 10^{-20} \, \mathrm{erg \, cm^{-2} \, s^{-1} Hz^{-1}}$.

2. The Samples

We consider both Lyman break and Lyman-α emission selected samples. For Lyman-α selection, we use the previously published sample from Pirzkal et al (2007; hereafter P07), which in turn is based on the HUDF emission line catalog of Xu et al (2007). This sample contains 9 Lyman-α-emitting galaxies, spanning redshifts $4.0 \leq z \leq 5.76$, line fluxes $2 \lesssim f/10^{-17} \, \mathrm{erg \, cm^{-2} \, s^{-1}} \lesssim 6$, and continuum magnitudes $25.5 \lesssim i \lesssim 29$.

For Lyman break selection, we derive new samples based on HUDF photometric pre-selection combined with GRAPES/PEARS grism spectroscopy. Because we have spectra for all objects in our sample, we can examine a more inclusive set of Lyman break galaxy candidates than is practical for photometric studies. We examined as candidate LBGs all objects having $V - i > 0.9$, and $i < 27.7$. The magnitude cut prevents the sample from being swamped by galaxies too faint for accurate photometry or spectroscopy. We inspected visually the GRAPES and PEARS spectra of all objects passing these selection cuts, and retained in our final sample those objects whose spectra support a Lyman break identification.

Table 1.   Properties of GRAPES/PEARS HUDF V-dropout Sample

Object ID	RA	Dec	i mag	$V - i$	$i - z$	B	Redshift	Grade
119	53.1660037	-27.8238734	27.51	2.14	-0.62	28.97	4.88	2.5
201	53.1649949	-27.8224088	27.59	1.23	-0.24	32.92	4.60	2
478	53.1733579	-27.8182711	27.06	1.11	-0.06	30.65	4.52	2
546	53.158038	-27.8179411	27.86	3.13	0.79	31.52	5.42	2.5
577	53.1614532	-27.8174379	27.08	1.01	0.09	30.55	3.8	2.5
646	53.1660559	-27.8167778	27.44	2.22	0.24	30.18	4.9	2
712	53.1783554	-27.8162519	27.26	2.32	0.13	32.4	5.12	1.8
1115	53.1722726	-27.8119732	26.40	1.85	0.17	28.89	4.72	1.8
1392	53.1563588	-27.8095883	27.75	3.96	-1.05	30.75	4.90	1
2408	53.1885357	-27.8034637	26.76	1.77	0.14	31.82	4.86	2
2599	53.1626689	-27.8022982	27.00	1.76	-0.07	29.75	4.88	2
2736	53.1499325	-27.8017358	26.94	1.39	0.11	32.27	4.56	2
2881	53.1415872	-27.8005681	25.84	1.78	0.18	29.79	4.56	2
2894	53.1462482	-27.8008077	27.58	2.57	-0.10	29.85	5.3	2
2898	53.1798203	-27.8008748	27.06	1.79	-0.32	29.50	4.67	2.3
3094	53.1514271	-27.7997637	25.72	1.18	0.02	29.57	4.62	1
3250	53.1326676	-27.7989430	27.14	3.74	-0.29	30.12	4.90	2.3
3968	53.1833331	-27.7959556	27.56	3.35	-0.82	31.55	4.7	2
5183	53.1437786	-27.7908654	27.38	0.91	-0.57	32.92	4.62	1
5225	53.1385743	-27.7902115	25.83	1.52	0.04	27.87	5.42	2
5296	53.1907601	-27.7903482	27.08	2.71	0.29	31.78	5.14	2.2
5307	53.1908538	-27.7903656	27.15	2.53	0.38	30.39	5.14	2.2
5788	53.1456573	-27.7882186	27.46	4.32	0.50	30.27	5.1	2
6066	53.1845519	-27.7869713	26.11	0.93	0.01	29.12	4.42	1
6139	53.1581263	-27.7863866	25.49	1.37	-0.11	31.51	4.68	1.2
6515	53.1273697	-27.7851656	27.15	1.25	-0.24	29.75	4.75	1
6681	53.1926615	-27.7841483	27.10	2.25	0.41	28.81	5.08	1.3
7050	53.1510392	-27.7828658	27.36	4.13	0.50	30.44	5.45	2.2
7352	53.1376954	-27.7812680	26.87	2.88	-0.02	29.37	5.04	2.5
8301	53.1671692	-27.7745246	27.18	2.91	0.22	32.47	5.0	2

To determine redshifts, we fitted our spectra with a model consisting of a power law continuum attenuated by Lyman-α forest absorption, which we modeled using the formalism of Madau (1995). We thus fitted three parameters to each spectrum: the flux normalization, spectral slope, and redshift. In cases with strong Lyman-α line emission, the fitted slope is strongly biased towards blue values, since we do not expliclitly fit emission lines.

We then assessed the best fitting model for each spectrum and assigned a grade to each. These grades were based on the χ^2 of the fit, the signal to noise in the spectrum, and a visual inspection of the fit. Grade 1 was given to the highest quality fits, where the LBG identification and redshift are very secure. Grade 2 was given to reasonably secure Lyman break objects. Grade 3 was given to sources that remain possible Lyman break objects but that cannot be confirmed, whether because the signal-to-noise was insufficient, or because the spectra suffered from contamination. Finally, grade 4 was assigned to photometric candidates that were refuted by the grism spectra. We assigned fractional grades to a modest number of galaxies where it seemed warranted.

In total, we considered 216 candidates fulfilling the photometric selection criteria. A few additional objects were examined in the early stages of the project, resulting in the inclusion in the final sample of two V dropouts (IDs 546 and 1392) having $27.7 < i < 27.9$. In total, we classified 39 objects as "good" ($1 \leq$ grade ≤ 2.5) Lyman break objects, 86 as refuted (grade 4) objects, and 94 as grade 3 ("unidentified"). Representative spectra for grades from 1 to 2.5 are shown in figure 1. The brightest confirmed Lyman break galaxies have $i \approx 25.5$. The fraction of grade 3 ("unidentified") sources rises steadily from 0 at $i < 25$ to 100% at $i \approx 27.7$. A very rough linear fit is $f \approx 0.3 + 0.2 \times (i - 26)$. Among those sources adequately classified using the grism spectra, the fraction confirmed as Lyman break galaxies *rises* weakly towards fainter magnitudes, from $\sim 25\%$ at $i \approx 25.5$ to $\sim 50\%$ at $i \approx 27.5$. To understand this, consider the primary contaminants of the photometrically selected Lyman break candidate lists. These are red stars in our Galaxy, and early type galaxies at intermediate redshifts. While the number-magnitude relation for Lyman break galaxies is steeply rising around $i \approx 26$, the number-magnitude relations for both contaminants are much flatter, and therefore the LBG fraction rises at the faint end.

The V dropout sample includes a range of morphologies, from simple, compact galaxies to extended sources with tails and/or multiple peaks (e.g., HUDF 5225; Rhoads et al 2005). Detailed morphological analysis of these and other high redshift UDF sources has been discussed by Pirzkal et al (2005, 2006).

Table 1—Continued

Object ID	RA	Dec	i mag	$V-i$	$i-z$	B	Redshift	Grade
8664	53.1890652	-27.7770042	26.77	2.08	0.08	29.9	4.9	1.3
8682	53.1888007	-27.7770931	25.62	1.94	0.06	28.70	5.08	2
8896	53.1900052	-27.7790544	26.92	1.56	0.09	31.30	4.33	2
9040	53.1711852	-27.7784585	25.97	3.42	-0.49	28.3	4.55	2
9057	53.1829957	-27.7804592	26.90	0.91	-0.02	31.84	4.17	2
9275	53.1531485	-27.766181	25.83	1.26	0.14	28.93	5.12	2
9777	53.1702387	-27.7628552	26.17	1.95	0.85	30.20	5.41	2.5
9983	53.1671627	-27.7598546	25.62	1.79	0.17	32.27	4.82	2
20191	53.1725558	-27.8137100	25.73	1.41	0.09	31.48	4.62	1

Note. — Properties of V dropout sources from GRAPES + UDF data. "ID" is the HUDF catalog number, since we used the HUDF catalog as the master object list for GRAPES. The "Grade" column indicates the quality of a candidate as assessed by visual inspection of the GRAPES and PEARS spectra. Objects assigned grade 1 are very secure Lyman break galaxies, while those assigned grade 2 are probable LBGs. Some objects are assigned non-integer grades between these possibilities. We also identified "grade 3" objects, for which our data could neither confirm nor refute a photometrically identified Lyman break candidate, and "rejected" objects, shown not to be Lyman break objects by their grism spectra. We do not tabulate these lower category sources.
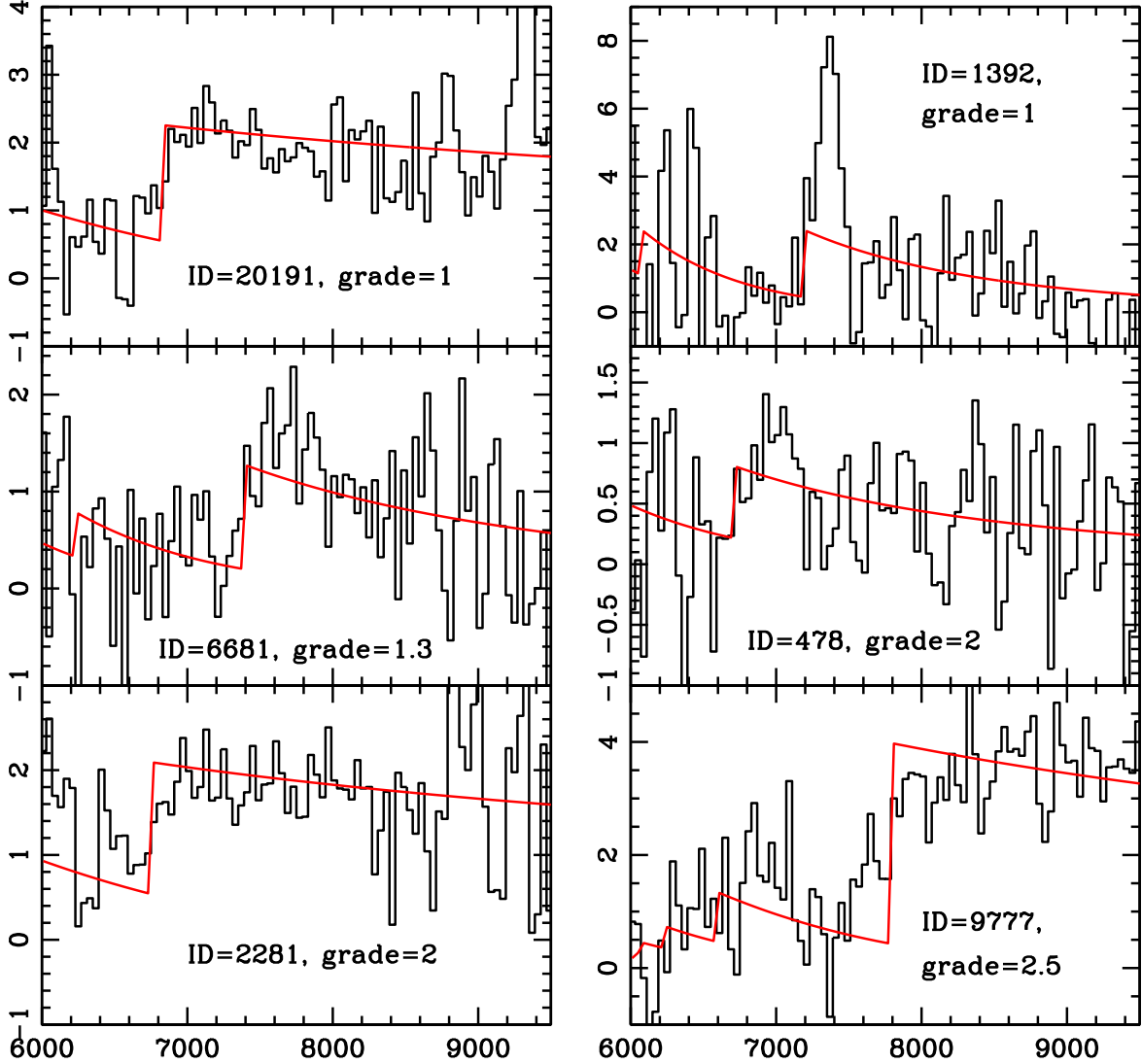
Fig. 1.— Six representative spectra from our HUDF V dropout sample. These span a range of quality, from grade 1 (best) to grade 2.5 (marginal). The grades were assigned by examination of both the 1D spectra (shown here after coadding all position angles) and the 2D spectra, in both cases examining both results from individual position angles and their average. The best fitting power law spectrum, attenuated by the IGM opacity based on Madau 1995, is overplotted. One of the plotted objects (1392) has a Lyman-α line, which is not included in the fitted model but which was used to establish the object's redshift.

3. Discussion

We compared our sample with the set of objects selected by the V dropout selection criteria that Giavalisco et al (2004) developed for the GOODS project. Those criteria are

$$[(V - i) > 1.5 + 0.9 \times (i - z) \quad \textbf{or} \quad (V - i) > 2.0]$$
$$\textbf{and} \quad (V - i) \geq 1.2 \quad \textbf{and} \quad (i - z) \leq 1.3 \ . \tag{1}$$

We used the same $i < 27.7$ magnitude cut when applying equation 1. Figure 2 illustrates both selection criteria in the $(i - z, V - i)$ color-color plane.

Of the 39 good Lyman break galaxies, 25 meet the Giavalisco et al selection criteria directly (eq. 1). One of these lies within 1σ of the selection region boundary, as do five objects that would narrowly fail the Giavalisco et al criteria. Thus, the photometric V-dropout criteria have a completeness of $\approx 25/39 = 64\%$ compared to the simple $V - i > 0.9$ cut of our spectroscopic sample. Most of the confirmed V-dropout LBGs missed by eq. 1 appear to be LBGs at a slightly lower redshift: Our color-redshift calculations indicate that a star forming galaxy should lie at $z \gtrsim 4.6$ to meet eq. 1, and $z \gtrsim 4.3$ to meet $V - i > 0.9$. These redshift boundaries will of course be blurred by variations in the galaxies' stellar populations, dust content, and Lyman-α line strength, all of which have some effect on galaxy colors. In practice, although only three of our spectroscopically measured redshifts actually fall at $z < 4.6$, there is a reasonable correlation between $V - i$ and redshift , and the inclusion of objects with $0.9 < V - i \lesssim 1.3$ does lower the mean redshift of the sample (see figure 4).

The reliability of the photometric criteria is broadly comparable. In total, we find 50 objects passing the criteria of eq. 1: The 25 confirmed Lyman break galaxies discussed above, plus 27 other sources *not* confirmed as Lyman break objects. Among these, 21 had inconclusive (grade 3) spectra, two are stars (grade-5), and only four are considered "refuted" with grade=4. Leaving aside the grade=3 sources, then, some $\approx 25/31 = 81\%$ of the objects that meet the photometric criteria are confirmed by inspection of their GRAPES/PEARS grism spectra. Combining this with the 64% completeness would naively imply that V drop galaxy counts derived directly from eq. 1 are slightly underestimated, by a factor of $0.64/0.81 \approx 0.8$.

The $i - z < 1.3$ color criterion in eq. 1 seems unlikely to strongly affect which galaxies are included in the sample. The reddest galaxy actually selected still has $i - z < 1$. Thus, if there are redshift $z \sim 5$ Lyman break objects with $i - z > 1.3$, they would have to form a disjoint population from the star-forming sample discussed in the present work. This cut does, however, help exclude L and T dwarfs from the sample.

A final point about sample selection is that Lyman break galaxies constitute only $14/165 = 8\%$ of those objects *failing* the Giavalisco et al criteria while still having $V - i > 0.9$ and $i < 27.7$. Thus, for a purely photometric criterion, eq. 1 is quite good, and in the absence of spectra we could not advocate a simple $V - i > 0.9$ selection. Expanding the selection region to include objects with $i - z \lesssim 0.2$ and $V - i > 0.9$ would be better than merely using $V - i > 0.9$ alone (since the $i - z$ cut eliminates many interlopers and no confirmed objects in our sample). This would increase the sample's completeness, but it would still reduce the overall reliability of the photometric selection when compared to the Giavaliso et al selection.

We show the redshift distribution of the V dropout sample in figure 3. The distribution shows no convincing structure beyond a broad maximum. In particular, we do not see any large scale overdensity akin to the one we reported at $z \approx 5.9$ based on the GRAPES i dropout sample (Malhotra et al 2005). The observed maximum spans $4.5 \leq z \leq 5.2$, and can be understood by considering the redshift-dependence of the selection criteria. At $z < 4.5$, the $V - i$ color is not red enough for the selection. At $z > 5.2$, reduction of the i-band flux by the Lyman-α forest is becoming significant.

We should expect the observed $V - i$ colors of the Lyman break objects to grow redder with increasing redshift, as the Lyman-α forest absorption shifts through the V bandpass. This effect is apparent in figure 4, though there is considerable scatter at each redshift.

3.1.   Lyman-α Emission Properties

With spectra of every Lyman break galaxy in the Hubble Ultra Deep Field, we can examine the statistics of Lyman-α emission from galaxies in our sample. We have previously published lists of emission line objects in the field (Xu et al 2007; Straughn et al 2008) and a more specific study of the Lyman-α galaxies, focussing on their ages, masses, and morphologies (Pirzkal et al 2007; hereafter P07).

Starting from the Lyman-α galaxy sample of P07 and the V-dropout Lyman break galaxy sample in this work, we find that five (ID numbers 712, 5183, 5225, 6139, and 9040) have previously identified Lyman-α emission lines. There are an additional four Lyman-α emitting galaxies in the P07 sample. Three of these (ID numbers 631, 9340, and 9487) are too blue to be included in our $V - i > 0.9$ sample, and the fourth (ID number 4442) is too faint for our $i < 27.7$ criterion. The P07 sample was based essentially on an emission line search combined with a stringent upper limit on B-band (435 nm) flux. The completeness of the emission line search is treated in Xu et al (2007). That sample is expected to be
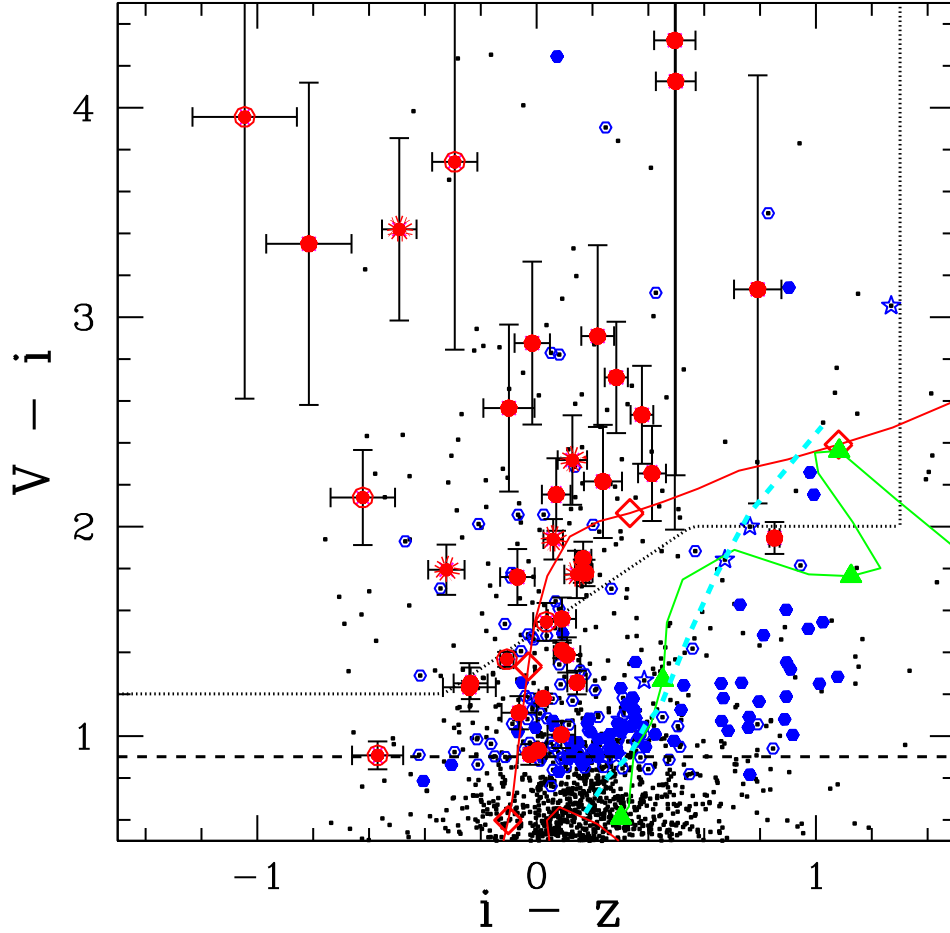
Fig. 2.— The color-color plane for V dropout selection. Small black dots show all objects in the parent catalog having $i < 29$ and i- and z-band magnitude errors < 0.3 mag. We examined the spectra of those objects with $V - i > 0.9$, $i < 27.7$, and $B > 27$. Those confirmed as Lyman break galaxies are shown as red circles with 1σ error bars. Among the confirmed sources, those with confirmed Lyman-α emission are circled, and those with suspected Lyman-α emission are marked by projecting "rays." Objects that were firmly rejected from the Lyman break sample (i.e., grade 4 objects) are shown as filled blue dots. Stars (from the list of Pirzkal et al 2005) are shown by open blue star symbols. Finally, candidates for which we have insufficient basis for judgment are shown as open blue circles. Candidates below the $V - i = 0.9$ line all lie within 1σ of that cutoff. We show the expected colors of star-forming galaxies at $4 \lesssim z \lesssim 6$ with a red line, and mark the colors for $z = 4.0, 4.5, 5.0,$, and 5.5 with open red diamonds. We show the colors of elliptical galaxies with $0 \leq z \lesssim 2$ as a green line, and mark redshifts $z = 0, 0.5, 1,$ and 1.5 with green triangles. A dashed cyan line marks the stellar locus, based on Pickles (1998) templates, from M6 (top) to K1(bottom). The dotted black line shows the selection region used by Giavalisco et al (2004; see text). The horizontal dashed line shows the expanded region covered by our $V - i > 0.9$ cut for inspection of spectra.
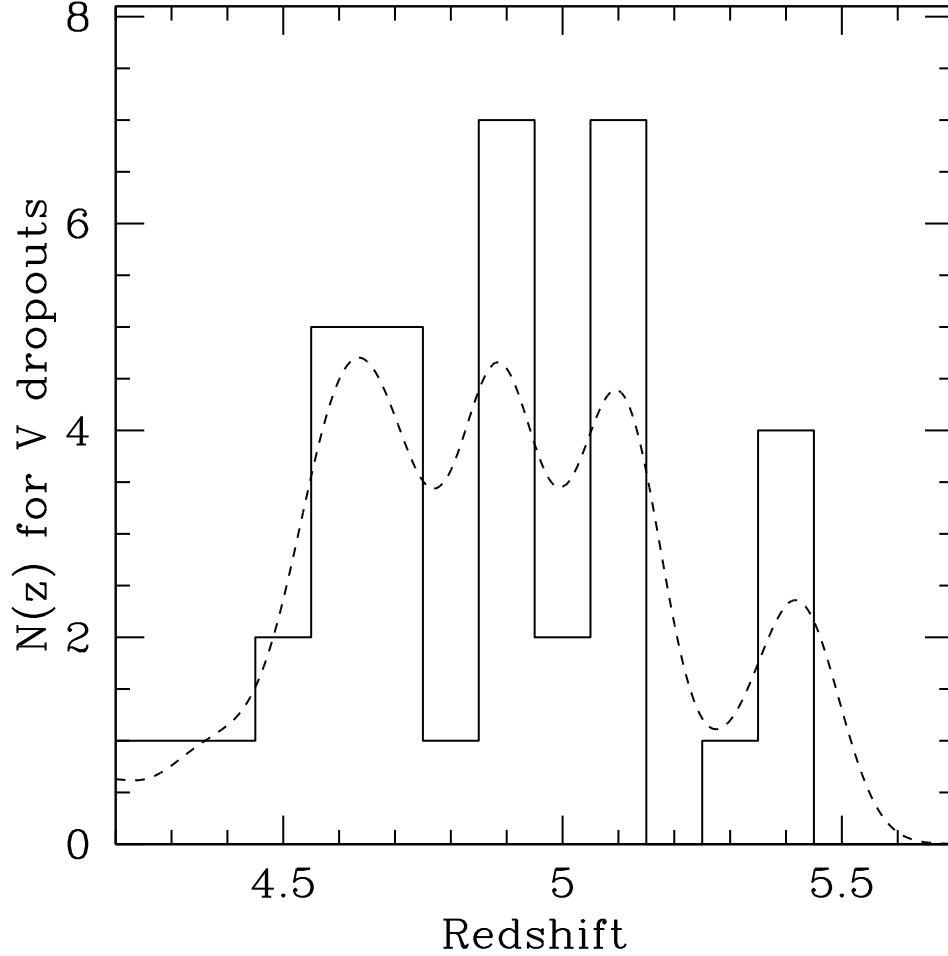
Fig. 3.— *Solid:* Histogram of V dropout galaxy redshifts, based on the $1 \leq$ grade ≤ 2.5 objects from table 1. *Dashed:* Generalized histogram of the same data, formed by adding Gaussians centered at the redshift of each object and having width $\sigma = 0.07$ (comparable to the redshift uncertainty for a "grade 2" object). The peaks in the distribution are not statistically significant.
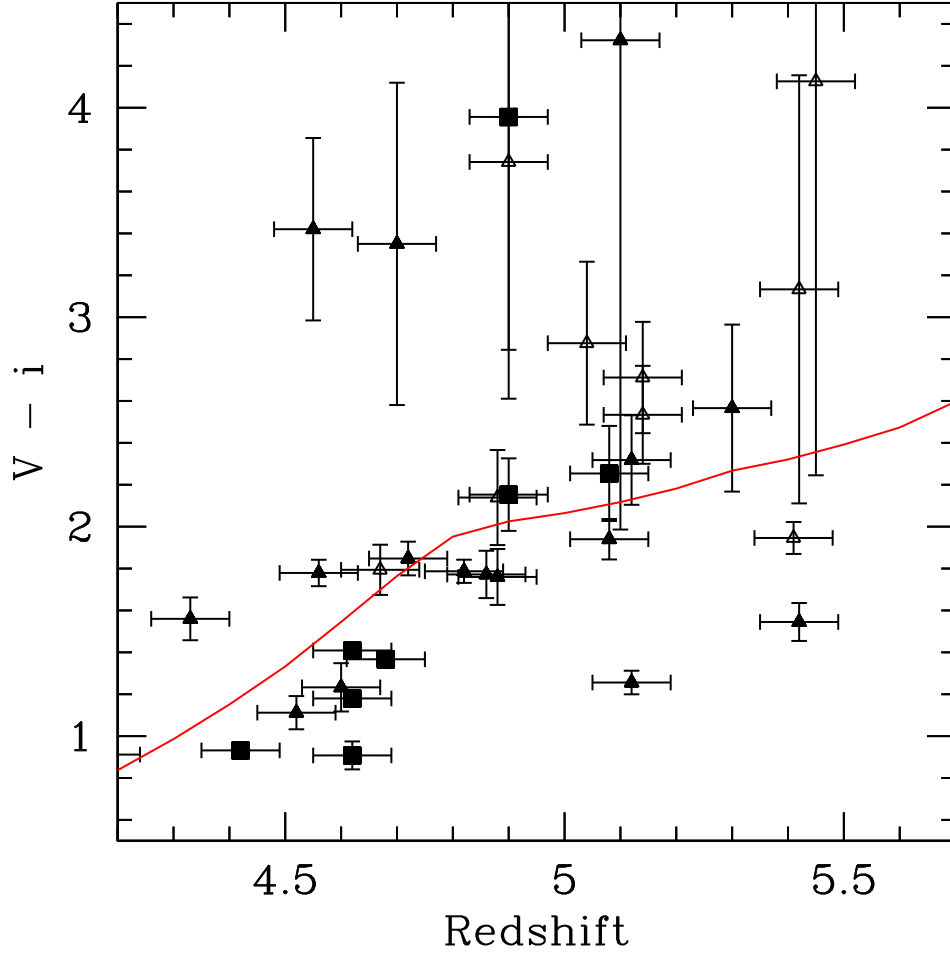
Fig. 4.— The redshift dependence of $V - i$ color for spectroscopically confirmed V-dropout Lyman break galaxies. The expected color of a template "Magellanic" spectrum is shown by the red curve. The inflection point at $z = 4.8$ corresponds to the redshift where the Lyman-α wavelength redshifts out of the V (F606W) filter and into the i (F775W) filter. Points at $z < 4.8$ that fall blueward of this fiducial line may in part be due to Lyman-α emission in the V filter. Point styles indicate the grade given to the Lyman break redshift fit: Heavy squares are the best fits (assigned grade < 1.5), filled triangles have grades between 1.5 and 2.1 (inclusive), and open triangles have grades between 2.1 and 2.5.

quite complete for Lyman-α galaxies that have $f_{Ly\alpha} \gtrsim 2 \times 10^{-17}\,\mathrm{erg\,cm^{-2}\,s^{-1}}$, $EW \gtrsim 120$Å, $4 \lesssim z \lesssim 6.5$, and $\theta_{FWHM} \lesssim 0.5''$. We conclude that $\sim 55\%$ of such Lyman-α emitting galaxies also pass our V dropout criteria. While the remaining Lyman-α galaxies are still well detected in the photometric catalog, many fail the dropout color criteria.

In addition to these previously identified Lyman-α objects, we find good visual evidence for Lyman-α emission in objects 1392, 2898, 3250, and 6515. Weaker evidence of a possible line is seen in 2408 and 8682. Object 119 also shows a clear emission line, which could be Lyman-α at $z = 4.88$. However, this line was interpreted in Xu et al (2007) as [O III] $\lambda\lambda 4959,5007$. (The ambiguity is linked to the object's faintness, $i \approx 27.3$, and we have assigned this object a grade of 2.5 to reflect the uncertainty in its redshift.) The detection of new Lyman-α emitters in the present paper is due to two factors. First, we have lower effective detection thresholds in line luminosity and/or equivalent width in the current work, because our line list includes objects identified by visual inspection of both 1-D and 2-D spectra in photometrically pre-selected high redshift galaxies. Thus, an emission line does not need as high a statistical significance to enter the present sample as was required in Xu et al (2007). Second, we are using not only the GRAPES data but also the PEARS-Deep data, nearly doubling the available data. This provides better statistical signal-to-noise ratio on most objects, and improved robustness to contamination by overlapping spectra thanks to the additional four position angles of data.

Combining all the detected Lyman-α lines, we infer a Lyman-α emission fraction in the range $9/39 = 23\%$ to $12/39 = 31\%$ for the V dropout sample.

There are two main ways in which HST grism searches can miss Lyman-α emission from well detected galaxies. First, the emission line is always located at the same wavelength as the continuum break introduced by Lyman-α forest absorption. This imposes a minimum observer-frame equivalent width that is comparable to the effective spectral resolution of the instrument. This spectral resolution, in turn, is set by the angular size of the target, given the slitless instrument.

Second, Lyman-α emission could come from a "photosphere" that is more extended than the star-forming regions that dominate the UV continuum light. There is a plausible physical mechanism for such extended Lyman-α emission, namely, resonant scattering of Lyman-α photons by neutral hydrogen in and around the emitting galaxy. Moreover, observations of Lyman-α "blobs" up to $\sim 10''$ in size (e.g Steidel et al 2000) provide direct evidence that Lyman-α can be scattered or emitted over wide spatial scales, at least in some rare objects. P07 report the effective radii in continuum emission for their sample of nine Lyman-α galaxies. Among these, six have sizes corresponding to $\lesssim 1.5$kpc FWHM, and the remaining three have sizes near 3kpc. If the typical Lyman-α photosphere is larger

(i.e. > 3kpc in extent), some Lyman-α lines would be missed in the slitless HST spectra, because their large spatial extent would translate to very broad line widths. 3kpc translates to $\sim 0.5''$, which in turn corresponds to a 400Å observed line width. Xu et al (2007) report a 70% detection completeness for 400Å lines, but this completeness drops (approximately linearly) to zero as the line width rises to 650Å (corresponding to $0.8''$ size).

To address this possibility, we stacked the 2-dimensional grism images of all 39 V-dropout galaxies, shifting them in wavelength to align the expected location of any Lyman-α emission in all spectra. All position angles were included in the average. The resulting average 2D spectrum is shown in figure 5. If spatially extended Lyman-α flux is prevalent in our sample, we should expect to see a region of diffuse emission at the Lyman-α wavelength. Moreover, the profile of this emission would be a fair representation of the "average" Lyman-α emission morphology. In practice, we see no evidence for extended Lyman-α emission in this figure. The continuum emission, a Lyman-α break, and weak transmitted flux through the Lyman-α forest region are all clearly detected. We also made a stack of the ten best Lyman-α emitters, and a stack of all the remaining 29 objects. The "Lyman-αstack" shows a clear emission line. Moreover, this line appears somewhat extended on visual inspection (figures 5 and 6). The difference is not highly significant, but a direct measurement of the spatial width of the spectrum yields FWHM=0.19" (or ≈ 1.3kpc) in the continuum region, and 0.26" (or ≈ 1.8kpc) in the line region.

As a quantitative test for extended Lyman-α, we have compared the spatial profile of the stacked spectrum (perpendicular to the dispersion direction) at both the Lyman-α location and in the adjacent continuum region. We find that the two profiles are indistinguishable (figure 6) . Thus, while we cannot rule out extended Lyman-α emission in a minority of cases, it is at most an exception to the rule, rather than a generic phenomenon in Lyman break galaxies. To place a quantitative upper limit on the flux in a spatially extended component, we first measure the 1σ noise level in the composite spectrum, which is about $1/3$ count/ksec/pixel. This corresponds to a flux level of $2 \times 10^{-18}\,\mathrm{erg\,cm^{-2}\,s^{-1}}$ in one $0.05''$ ACS WFC pixel. If we co-add the results for a larger solid angle Ω, we expect the limit to scale as $\sqrt{\Omega/\Omega_{pix}} = \sqrt{N_{pix}}$. We define two sets of pixels, each consisting of two $1.05'' \times 0.3''$ rectangular regions and so totaling $0.63\square''$, and each excluding a strip $0.3''$ wide along the trace of the stacked spectrum. The first set of pixels is centered at the expected location of Lyman-α emission, while the second is centered $1.05''$ away, towards the red end of the spectrum. We take the total fluxes in these two sets of pixels, apply the wavelength-dependent sensitivity conversion factor, and compare the results. In the region where diffuse Lyman-α might be expected, we find a formal flux excess of $(5 \pm 4) \times 10^{-17}\,\mathrm{erg\,cm^{-2}\,s^{-1}}$. This is comparable to the typical fluxes of ground-based narrowband Lyman-α surveys.
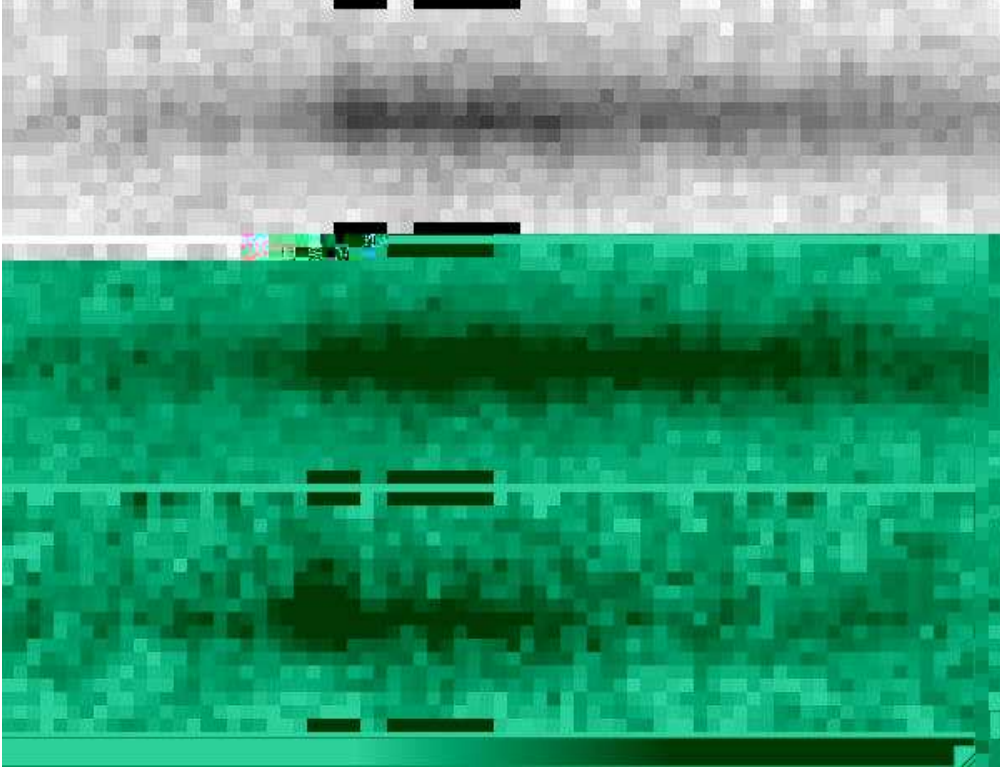
Fig. 5.— 2-dimensional stacks of V dropout grism data. *Top:* The full V dropout sample. *Middle:* Those objects *without* individually detected Lyman-α emission. *Bottom:* Those objects *with* individually detected Lyman-α emission. Each stack is performed using rectified, wavelength calibrated grism stamps. We used a "shift and add" algorithm. We see a Lyman-α line in the first and third stacked spectra, but no strong evidence for diffuse, extended Lyman-α emission in the rest of the population. The pixel scale is 40Å (observer frame) in the spectral direction, and 0.05" in the spatial direction. The expected location of Lyman-α, and comparison region of the continuum spectrum, are marked by solid bars at the edges of each spectrum. These regions are used to produce the spatial profiles in figure 6. Because there is a range of redshifts in the sample and we have stacked the images using observer frame wavelengths, there is no unique pixel - wavelength correspondence away from 1215Å. We adopted this approach because the observed Lyman-α profile then corresponds directly to the size of the Lyman-α emitting region of the sample galaxies. The approximate total exposure times in the three stacks are 8.5×10^6, 6.2×10^6, and 2.3×10^6 seconds respectively.
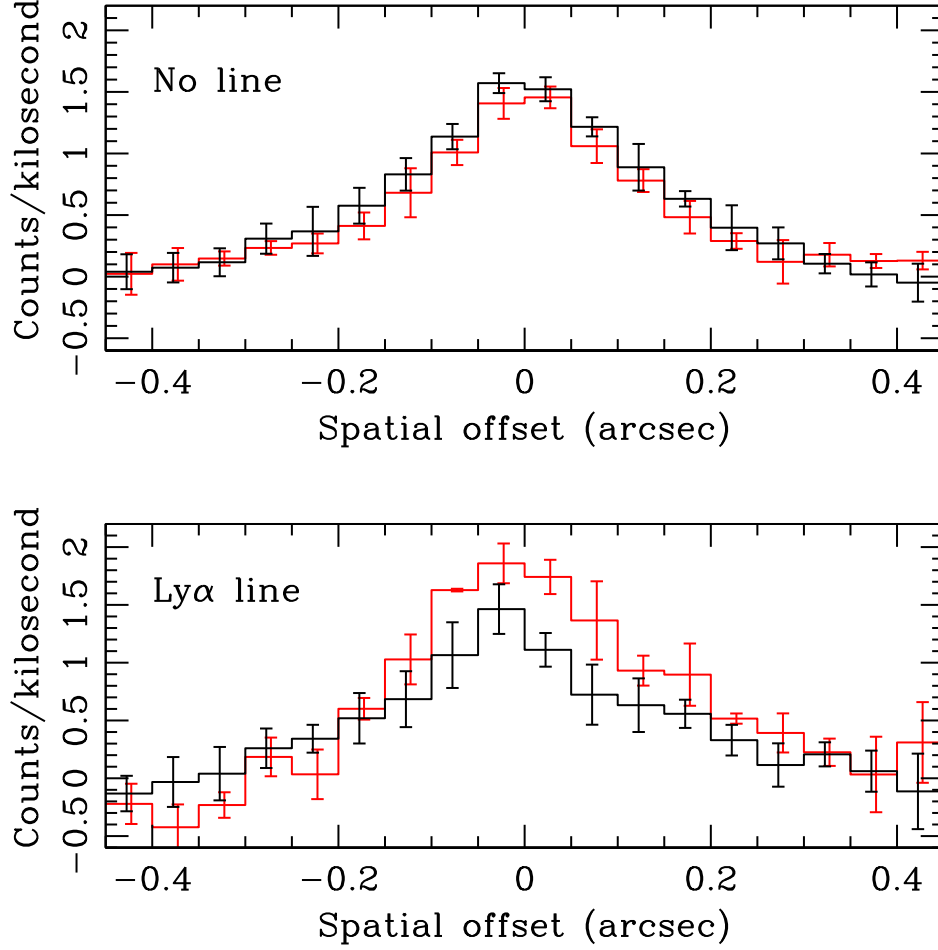
Fig. 6.— Here we compare spatial profiles of the composite V-dropout spectrum (fig. 5) at the Lyman-α line wavelength (red line) and the adjacent continuum at ≈ 1280Å rest frame (black line). The two profiles for the "no line" stack are indistinguishable within their combined 1σ error bars, implying that there is no substantial diffuse Lyman-α component in this stacked spectrum. The stack for the "Lyman-α line" sample *does* suggest that Lyman-α comes from a modestly larger region than the starlight in galaxies with prominent Lyman-α lines, although the statistical significance of the result is low with present data.

4.   Summary

We have examined GRAPES and PEARS spectra of 216 photometrically selected candidate Lyman break galaxies, and spectroscopically confirmed 39 of them. Our pre-selection used a wider range of color space ($V - i > 0.9$) than more traditional "V-dropout" Lyman break color criteria, in order to assess the completeness of those criteria, along with their reliability. We find that 64% of our confirmed objects meet the traditional criteria. Among those galaxies passing the traditional criteria, and having adequate spectra for classification, we find that 81% are confirmed as Lyman break galaxies. Our V drop sample includes 55% of Lyman-α emitting galaxies previously identified in this redshift range using GRAPES data (Xu et al 2007, Pirzkal et al 2007). The "missing" Lyman-α galaxies are either too blue in $V - i$ (in part due to the emission line in the V filter) or too faint in the continuum for our V dropout selection criteria. We also detect 4–7 additional Lyman-α galaxies not included in the earlier samples. Our overall Lyman-α detection fraction is comparable to that in spectroscopic followup of other Lyman break surveys (e.g., Steidel et al 2000). We have examined our stacked 2D spectra for evidence of the diffuse Lyman-α emission that might result from resonant scattering of Lyman-α photons in neutral hydrogen near young galaxies. In the overall stack of 39 galaxies, we find no significant evidence for such emission down to a 2σ upper limit of $9 \times 10^{-17}\,\mathrm{erg\,cm^{-2}\,s^{-1}}$ over an $0.6\square''$ region. On the other hand, when we examine the composite spectrum of just those galaxies with individually identified Lyman-α lines, we see a modestly broader spatial profile at the wavelength of Lyman-α than in the adjacent continuum. This is consistent with the possibility that scattering of Lyman-α photons results in a somewhat extended Lyman-α photosphere in these objects.

REFERENCES

Beckwith, S. V. W., et al. 2006, AJ 132, 1729

Ferguson, H. C., et al. 2004, ApJ 600, L107

Giavalisco, M., et al. 2004, ApJ 600, L103

Hathi, N. P., Malhotra, S., & Rhoads, J. E. 2008, ApJ 673, 686

Madau, P. 1995, ApJ 441, 18

Malhotra, S., et al. 2005, ApJ 626, 666

Malhotra, S., et al 2008, in preparation

Pickles, A. J. 1998, PASP, 110, 863

Pirzkal, N. et al. 2004, ApJS 154, 501

Pirzkal, N., Malhotra, S., Rhoads, J., & Xu, C. 2005, BAAS 207, 22.16

Pirzkal, N., Sahu, K. C., Burgasser, A., Moustakas, L. A., Xu, C., Malhotra, S., Rhoads, J. E., Koekemoer, A. M., Nelan, E. P., Windhorst, R. A., Panagia, N., Gronwall, C., Pasquali, A., & Walsh, J. R. 2005, ApJ 622, 319.

Pirzkal, N., Xu, C., Ferreras, I., Malhotra, S., Mobasher, B., Rhoads, J. E., Pasquali, A., Panagia, N., Koekemoer, A. M., Ferguson, H. C., & Gronwall, C. 2006, ApJ 636, 582.

Pirzkal, N., Malhotra, S., Rhoads, J. E., & Xu, C. 2007, ApJ 667, 49

Rhoads, J. E., et al. 2005, ApJ 621, 582

Spergel, D. N., et al. 2003, ApJS, 148, 175

Spergel, D. N., et al. 2007, ApJS, 170, 377

Steidel, C. C., Adelberger, K. L., Shapley, A. E., Pettini, M., Dickinson, M., & Giavalisco, M. 2000, ApJ 532, 170

Straughn, A., et al 2008, AJ, submitted.

Xu, C., et al 2007, AJ 134, 169